

Facile Synthesis of Zn-TiO₂ Nanostructure, Using Green Tea as an Eco-Friendly Reducing Agent for Photodegradation of Organic Pollutants in Water

Tavakoli, F. and Badiiei, A^{*}

School of Chemistry, College of Science, University of Tehran, Tehran, Iran

Received: 08.02.2018

Revised: 20.05.2018

ABSTRACT: The present study synthesizes Zn-TiO₂ photocatalyst via a simple and economic green route, in which Green Tea is applied as a green reducing agent due to the presence of polyphenols molecules. Polyphenol molecules in green tea act as a reductant, thus changing Zn²⁺ to metallic Zn. The by-produced nanocomposites are characterized by using XRD, FESEM, EDS, and DRS. Zn-TiO₂ photocatalyst possesses great efficient charge separation properties. In order to investigate the presence of Zn, different weight ratio of Zn to TiO₂ (viz. 5 wt%, 10 wt%, 15 wt%, 20 wt%, 25 wt%, 30 wt%, 35 wt%, 40 wt%, 45 wt%, and 50 wt%) have been synthesized and their performance in Acid Orange 7 (AO7) photodegradation, compared with pure TiO₂. According to the results, the compound with 25 wt% Zn shows 97% degradation of AO7 as a model pollutant. Also, it has been shown that after three tests with EDTA, benzoic acid, and under Ar gas, photodegradation of AO7 with Zn-TiO₂ photocatalyst mainly depends on photogenerated holes.

Keywords: Zn-TiO₂; Green Synthesis; Green Tea; Photocatalyst; Acid Orange 7.

INTRODUCTION

Water is essential to life, being especially necessary for human beings, first for his food, then for his health, and finally for his agricultural and industrial activities (Shen et al., 2010). Consequently, human population's settlement on earth is based on freshwater resources. In order to degrade organic pollutants effectively, TiO₂-based photocatalysts have been widely investigated as a disinfection agent in the past few decades (Sabet & Salavati, 2012; Sabet & Salavati, 2014; Sangsefidi et al., 2016; Sabet & Salavati, 2015; Sabet & Jahangiri, 2017; Ayni, 2016). The TiO₂ nanoparticles have been used for photodegradation of organic pollutants, thanks to their extraordinary optical

properties (Shiravand, 2012; Eskandarloo & Badiiei, 2016a; Eskandarloo & Badiiei, 2016b). The photocatalytic degradation mechanism of TiO₂ nanoparticles has been addressed in many papers (Fujishima, 2008; Hashimoto, 2005; Roig, 2003; Neelakandeswari, 2011; Masoumi, 2016). However, its application is limited due to its narrow photocatalytic region ($\lambda < 400$ nm) and ability to absorb a small fraction of incident solar irradiation and indoor light, resulting from its relatively large band gap (anatase, ~3.2 eV). Furthermore, the rapid recombination of electrons and holes is one of the main reasons for low photodegradation efficiency of TiO₂ (Malato, 2009; Xu, 2011; Xie, 2010; Nayak, 2011). Several methods can improve photocatalytic performance of

* Corresponding Author, Email: abadiei@ut.ac.ir (A. Badiiei)

TiO₂ nanoparticles, e.g. doping of carbon, metals, and nonmetals along with surface organic modification. Therefore, the doping of TiO₂ and metals such as Ag, Cu, Zn, Au, etc. is promising to improve photocatalytic performance of TiO₂ due to enhancing the photoinduced charge transfer (Lin, 2007; Wang, 2007).

Recently, there has been great effort to use green and environmentally-friendly methods for synthesis of nanosized materials, which involves the use of plant or fruit extracts as a stabilizer, reducing agent or capping agent to control crystal growth (Tavakoli & Salavati, 2013; Tavakoli & Salavati, 2015). Here, we use Green Tea as a natural reducing agent to synthesize Zn-TiO₂ to demonstrate a green and economic method for preparation of Zn-TiO₂. Green Tea is a rich source of polyphenols molecules. Plants with polyphenols can act as reducing agent, thus they have antioxidant property. Some of these plants can be used in the synthesis of nanoparticles due to the presence of polyphenols such as catechins, flavonols, flavanones, phenolic acid, and glycosids. Examples of plants, capable of acting as reducing agent, include pomegranate, cerasus pranus, mulberry, green tea, garlic, etc. Polyphenols are water-soluble vacuolar molecules. Odorless and nearly flavorless, they contribute to the taste as a moderately astringent. No wonder that they manage to reduce Zn²⁺ to metallic Zn. In this work, Zn-TiO₂ compound has been prepared through coprecipitation and then thermal method in the presence of Green Tea as reducing agent. The photocatalytic performance of this compound has been investigated for photodegradation of acid orange 7 (AO7) as a pollutant model. In order to check the presence of Zn metal in photodegradation performance of AO7, bare TiO₂ have been tested in the photodegradation of AO7. On the other hand, the weight ratio of Zn in TiO₂ as a crucial effect on photodegradation performance has been investigated and the

by-produced Zn-TiO₂, characterized by means of XRD, FESEM, TEM, EDS, and DRS.

MATERIAL AND METHODS

All reagents for synthesis of Zn-TiO₂, such as zinc nitrate and titanium dioxide, were purchased from Merck and employed without any further purification. The Green Tea was obtained from Lahijan, Iran. The synthesis was carried out at atmospheric pressure and ambient temperature with an ultrasonic irradiation, provided by a probe sonicator (Qsonica Q700, Newtown, CT, US). FT-IR spectra, ranged between 400 and 4000 cm⁻¹ on Rayleigh WQF-510a spectrometer. Patterns of Powder X-ray Diffraction (XRD) were collected from a diffractometer, made by Philips Company with X'pertpro monochromatized Cu K α radiation ($\lambda = 1.54 \text{ \AA}$). Microscopic morphology of products was visualized by SEM (MIRA3 TESCAN). TEM images were obtained on a CM30 transmission electron microscope with an accelerating voltage of 300 kV. Energy Dispersive Spectrometry (EDS) analysis was studied by XL30, Philips microscope with the sample's DRS obtained by means of AvaSpec 2048 TEC spectrometer in order to determine the optical band gap (E_g) of Zn-TiO₂ compound. For determination of the E_g Eq. (1) was used:

$$\alpha(h\nu) = B(h\nu - E_g)^{1/2} \quad (1)$$

where α is optical absorption coefficient; B, a constant dependent on transition probability; h , the Plank's constant; and ν , the radiation frequency. The E_g values were calculated by plotting $(\alpha h\nu)^2$ versus $h\nu$, followed by extrapolation of the linear part of the spectra to the energy axis.

Zn-TiO₂ nanostructures were prepared by the following experimental sequence: Firstly, a certain amount of zinc nitrate was added drop by drop into TiO₂ solution (i.e., 2gr of TiO₂ dispersed in 50 mL of distilled water) under ultrasonic irradiation,

followed by 50ml Green Tea (20gr green tea in 50 ml water) to be added into the above solution, again in drops. The obtained mixture was stirred at room temperature for 12h and the resultant precipitates were filtered, washed with distilled water and absolute ethanol, and dried at 60°C in vacuum. Finally, the product was treated at 450°C under Ar gas. The experiment was carried out by using 5wt%, 10wt%, 15wt%, 20wt%, 25wt%, 30wt%, 35wt%, 40wt%, 45wt%, and 50wt% of Zn to TiO₂ at the same conditions, respectively.

The photocatalytic degradation processes were carried out at room temperature in a batch quartz reactor. Artificial irradiation was provided by an 8W (UV-C) mercury lamp (Philips, Holland), which emitted around 254 nm, positioned on top of the batch quartz reactor. In each run, 40 mg of the catalyst was dispersed in 100 ml water. Afterwards, the desired concentration of AO7 (20 mg.L⁻¹) and photocatalyst (400 mg.L⁻¹) were transferred into the batch quartz reactor to be stirred for 30 min and reach the adsorption equilibration in the dark before irradiation. The photocatalytic reaction was initiated by turning on the light source. At given irradiation time intervals, the samples (5 ml) were retrieved, centrifuged (Sigma 2-16p), and then the AO7 concentration was analyzed by UV-vis spectrophotometer (Rayleigh UV-1600) at λ_{max} = 485 nm. All experiments were performed at initial pH of dye solution (pH = 6.1). The degradation efficiency was calculated by Eq. (2):

$$\text{Degradation efficiency (DE (\%))} = \frac{(C_0 - C_t/C_0) \times 100}{(2)}$$

where C₀ and C are concentrations of AO7 (mg.L⁻¹) at the time 0 and t, respectively.

RESULTS AND DISCUSSION

Fig.1 (a, b) shows the XRD pattern of TiO₂ and Zn-TiO₂. According to Fig.1a, for the TiO₂ compound, the XRD diffraction

reflections at 2θ of 25.8°, 38°, 39.5°, 48°, 55°, 62.6°, 69.7°, and 75.7° can be indexed to the characteristic reflections of (101), (004), (112), (200), (211), (213), (220), and (215) plane reflections of anatase crystal structure TiO₂. On the other hand, XRD pattern of Zn-TiO₂ shows the reflections at 2θ of 24.7°, 35.1°, 38.4°, 39.3°, 48.1°, 54.5°, 62.6°, 69.7°, and 75.7°, corresponding to (101), (202), (004), (112), (200), (204), (213), (220), and (215), respectively. The reflections at 2θ of 35.1° and 54.5° were due to the presence of Zn on the surface of anatase TiO₂. Since the metal was doped during the TiO₂ synthesis process, resulting in a difference of ionic radius between zinc and titanium ions (which accounted to 0.74Å and 0.068nm, respectively), TiO₂ crystalline structure became defective. As the cations got exchanged with one another, TiO₂ had cationic defect. In some cases, by adding a metal, the anatase phase of TiO₂ is converted into a rutile phase, though this phenomenon did not happen here, according to the XRD pattern of TiO₂ and Zn-TiO₂.

Fig. 2 shows the SEM and SEM mapping images of TiO₂ and Zn-TiO₂. According to SEM images, the best distribution of Zn metals belonged to the surface of spherical TiO₂, whereas SEM mapping confirmed the presence of Zn on TiO₂ surface.

Fig. 3 shows the TEM image of TiO₂ and Zn-TiO₂ compounds, according to which, Zn nanoparticles had been well distributed on TiO₂ nanoparticles. As shown in TEM images, the particle size of TiO₂ and Zn nanoparticles were (80-120) nm and (20-30) nm, respectively.

In order to get information on the elements, the Zn-TiO₂ compound was examined by EDX analysis, illustrated in Fig. 4. In the EDX spectrum of Zn-TiO₂ composite, the main elements such as Ti, O, and Zn were presented. According to EDX analysis, the existence of Zn nanoparticles on the surface of TiO₂ can be confirmed.

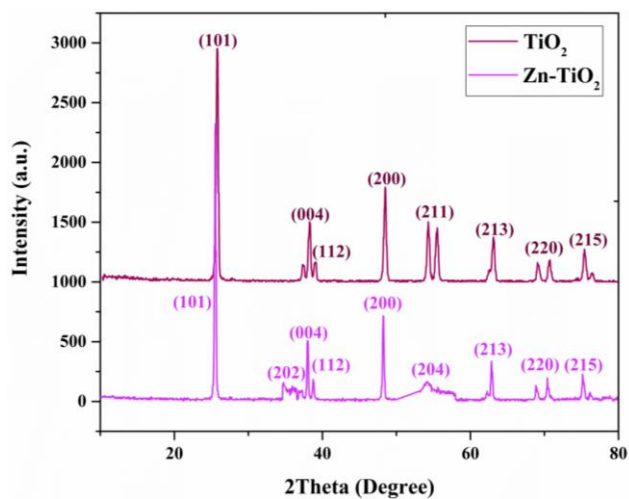


Fig.1. XRD pattern of TiO_2 and Zn-TiO_2 compounds

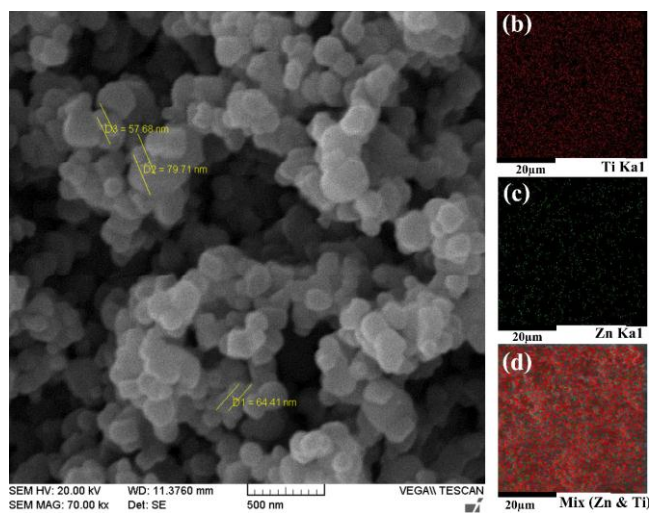


Fig. 2(a) SEM images of Zn-TiO_2 , (b), (c) and (d) SEM mapping images of Zn-TiO_2

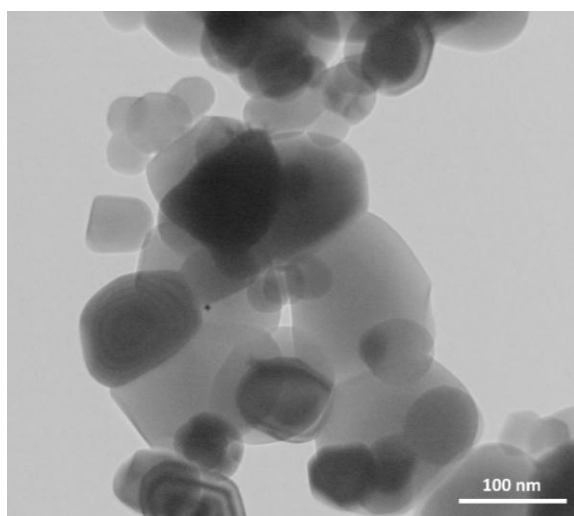


Fig. 3. TEM image of (a) TiO_2 and (b) Zn-TiO_2

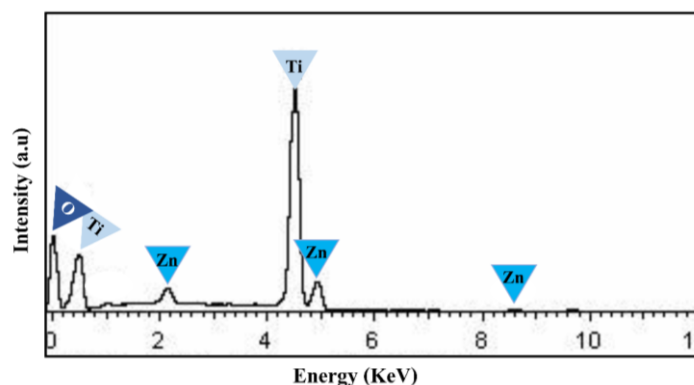


Fig. 4. EDX spectra of Zn-TiO₂

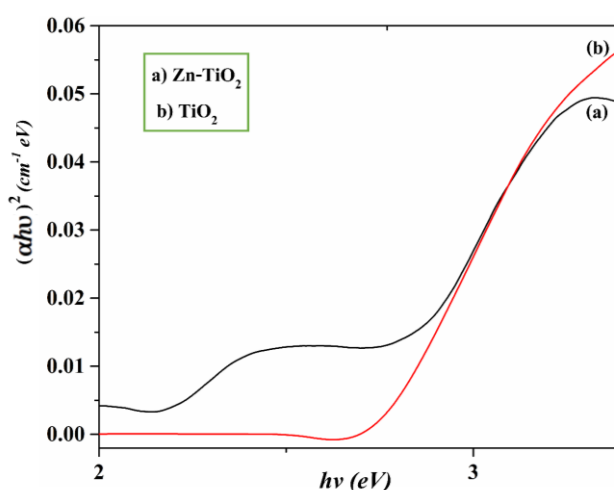


Fig. 5. Diffuse Reflectance Spectra (DRS) of (a) Zn-TiO₂ and (b) TiO₂

UV-visible, diffused reflectance spectra of TiO₂ and Zn-TiO₂ can be observed in Fig. 5. The calculated band gap energies of TiO₂ and Zn-TiO₂ were 2.9 and 2.65 eV, respectively. The slight reduction in the band gap of Zn-TiO₂ nanostructures implies that unpaired π electrons from Zn may bond with free electrons of TiO₂.

So the calculated band gap of Zn-TiO₂ was about 2.65, indicating that of the band gap of TiO₂ did narrow down and this narrowing should be attributed to the Ti-O-Zn bonds. Electrons have a tendency to flow from higher to lower Fermi levels in order to adjust the Fermi energy levels. The calculated conduction band position of anatase TiO₂ was about -4.21 eV with a band gap of about 2.9 eV, zinc can accept the photoexcited electrons from TiO₂. Thus, the photoinduced electron-hole pairs

got effectively separated and the probability of electron-hole recombination was decreased.

The valence band (VB) and conduction band (CB) potentials of semiconductors are two important factors for effective separation of photogenerated electron-hole pairs to generate OH radicals and superoxide anions. The VB and CB potential edges were calculated, using the following empirical formula (Eskandarloo & Badiei, 2014; Huang, 2013):

$$E_{VB} = X - E^e + 0.5 (E_g)$$

$$E_{CB} = E_{VB} - E_g$$

where E_{VB} and E_{CB} are the valence and conduction band edge potentials of a semiconductor, respectively; X, the electronegativity value of the semiconductor that is the geometric mean

of the electronegativities of constituent atoms; E^e , the energy of free electrons on the hydrogen scale (~ 4.5 eV); and E_g , the band gap energy of the semiconductor.

Overall mechanism for the formation of Zn^0 via polyphenols in green tea can be seen in the equation below, in which Ar represents the aromatic ring and n stands for the number

of groups, oxidized by Zn^{2+} .



The photocatalytic performance of Zn-TiO₂ and bare TiO₂ hybrid were investigated, using aqueous AO7 dye as a model compound under UV light irradiation.

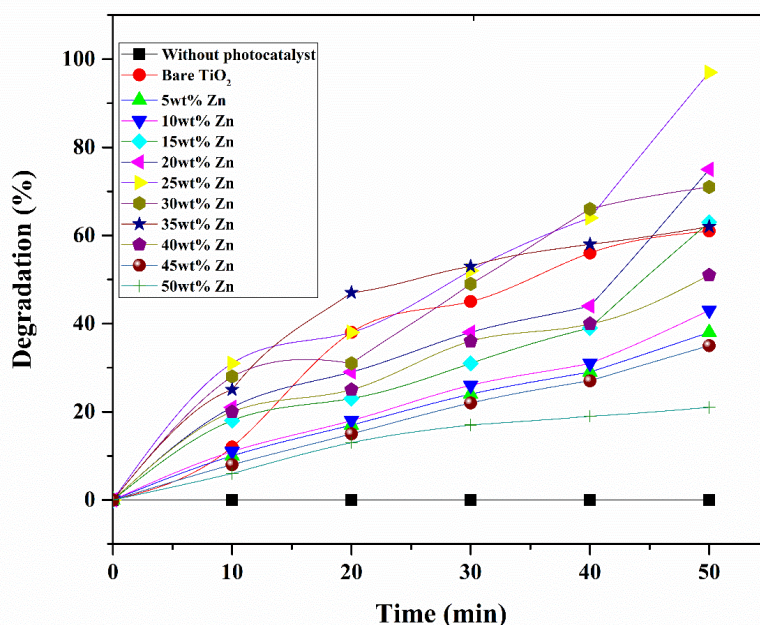


Fig. 6. Degradation curve of AO7 aqueous dye with UV light without photocatalyst, TiO₂, and different weight ratio of Zn to TiO₂

As shown in Fig. 6, when the only AO7 dye was exposed to UV light, no degradation of AO7 was observed. According to this observation, degradation of AO7 is only due to the presence of the photocatalyst. In order to evaluate the effect of Zn loading, different weight ratios of Zn (viz. 5wt%, 10wt%, 15wt%, 20wt%, 25wt%, 30wt%, 35wt%, 40wt%, 45wt%, and 50wt%), loaded on TiO₂ photocatalyst, were prepared and their photocatalytic performance tested as well (Fig. 6). The sample with 25wt% Zn showed higher photocatalytic degradation, compared to pure TiO₂ nanoparticles, while 5wt% and 50wt% Zn-loaded TiO₂ photocatalyst decreased the photocatalytic activity. As shown in Fig. 6, by increasing the weight ratio of Zn to TiO₂, the photocatalytic

performance of coupled nanoparticles for AO7 degradation was decreased. The first reason for the reduction in photodegradation was that higher loading of Zn could increase the recombination rate of electrons and holes, thus preventing the charges from getting separated. The second reason was that higher loading of Zn may decrease the active sites of TiO₂ and adsorptivity of coupled nanoparticles for adsorbed dye molecules on the surface of TiO₂, thereby affecting the photocatalytic performance and preventing the light from arriving at active sites of TiO₂. It can be seen in Fig. 6 that TiO₂ with 25wt% Zn exhibits 97% AO7 degradation within 50 min, though only 61% of degradation was shown in the presence of bare TiO₂. Generally, in order to evaluate the

photocatalytic performance of Zn-TiO₂ coupled nanoparticles, several samples with different weight ratios of Zn were synthesized and their performance in AO7 photodegradation was investigated. According to Fig. 6, by increasing the weight ratio of Zn from 5 wt% to 10 wt%, 15 wt%, 20 wt%, and 25 wt%, photodegradation was increased from 38% to 43%, 63%, 75%, and 97%, respectively; however, increasing this parameter from 25 wt% to 30wt%, 35wt%, 40wt%, 45wt%, and 50 wt%, photodegradation plummeted

from 97% to 71%, 62%, 51%, 35%, and 21%, respectively. According to these results, the weight ratio of Zn was a crucial factor for AO7 photodegradation.

In general, during photocatalysis, hydroxyl radicals, superoxide anions (O₂⁻), and holes (h⁺) are the reactive species for degradation of organic pollutants. In order to understand the photocatalytic activity of Zn-TiO₂ compound for AO7 degradation, a series of free radicals trapping experiments were carried out, as shown in Fig. 7.

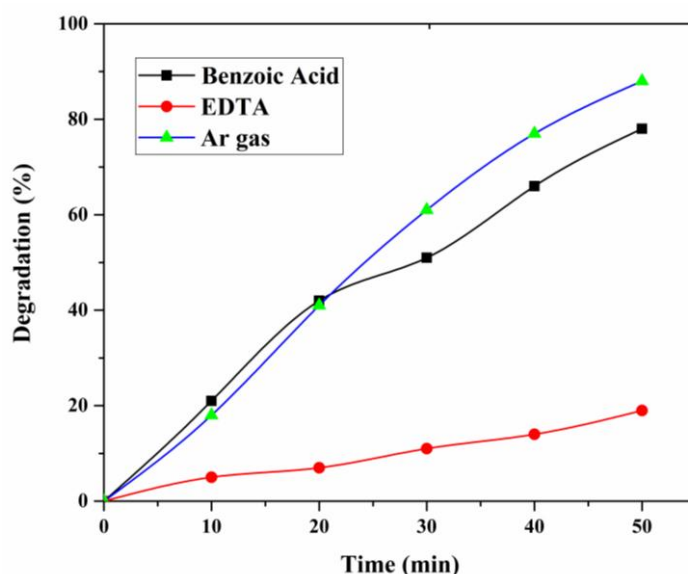


Fig. 7. Series of trapping experiments (a) Benzoic Acid ,(b) EDTA, and (c) Ar gas for AO7 degradation during Zn-TiO₂ photocatalysts under UV6 light irradiation

In the presence of a hydroxyl radical scavenger such as benzoic acid (0.5mM), as much as 78% degradation was observed. In case of benzoic acid, only 19% degradation was decreased than that of the scavenger-free photocatalytic system for AO7, as shown in Fig. 7, clearly suggesting that photocatalytic degradation of AO7 dye was not mediated through OH radical reaction, solely. In order to further examine the exact reactive species, involved in AO7 degradation, 10ml EDTA (0.01M), as an effective h⁺ scavenger got added into the AO7 reaction solution. The rate of AO7 degradation was drastically suppressed, i.e. only 19% of AO7 degradation was noticed (Fig. 7b), which

confirmed that the photoinduced holes (h⁺) were one of the main reactive species for AO7 degradation. In order to further prove the degradation process, induced by photogenerated electrons in photocatalytic degradation of AO7, another experiment was performed under Ar atmosphere (Fig .7c) . High purity Ar gas was continuously purged throughout the reaction process under an ambient condition ,which eliminated the dissolved oxygen content from the reaction solution ,thereby preventing the formation of O₂⁻. As a result ,88% of AO7 degradation was observed after 50 min of UV light illumination, instead of 97% in a normal atmospheric condition. This reduction in the

degradation percentage (~9%) in the presence of Ar gas shows that $O_2^{\cdot-}$ radicals were not reactive species for AO7 degradation, clearly emphasizing that AO7 degradation mainly depended on photogenerated holes only.

Fig. 8 shows the graphical abstract for green synthesis of Zn-TiO₂ via Pomegranate as a green reducing agent and

photocatalytic performance of Zn-TiO₂ photocatalyst in degradation of AO7 as an organic pollutant in water.

Mineralization of AO7 during the photocatalytic degradation in the presence of Zn-TiO₂ nanoparticles was studied through disappearance of UV-vis with Fig. 9 illustrating the changes in the UV-vis.

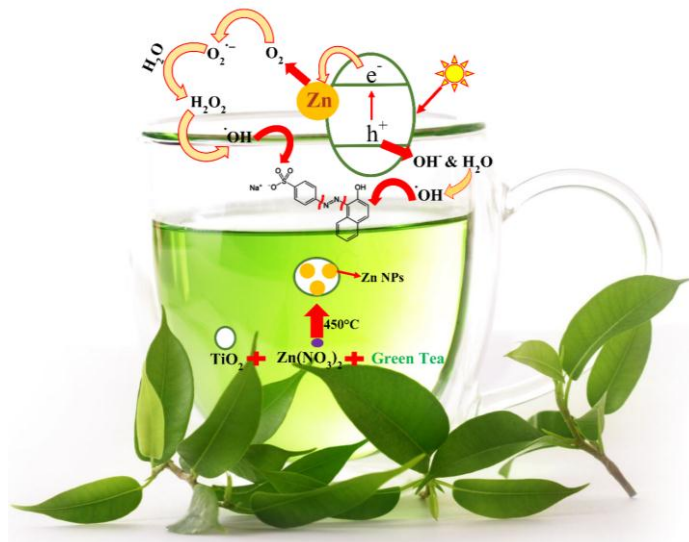


Fig. 8. graphical abstract for green synthesis of Zn-TiO₂ via pomegranate as a green reducing agent and photocatalytic performance of Zn-TiO₂ photocatalyst in AO7 degradation as an organic pollutant in water

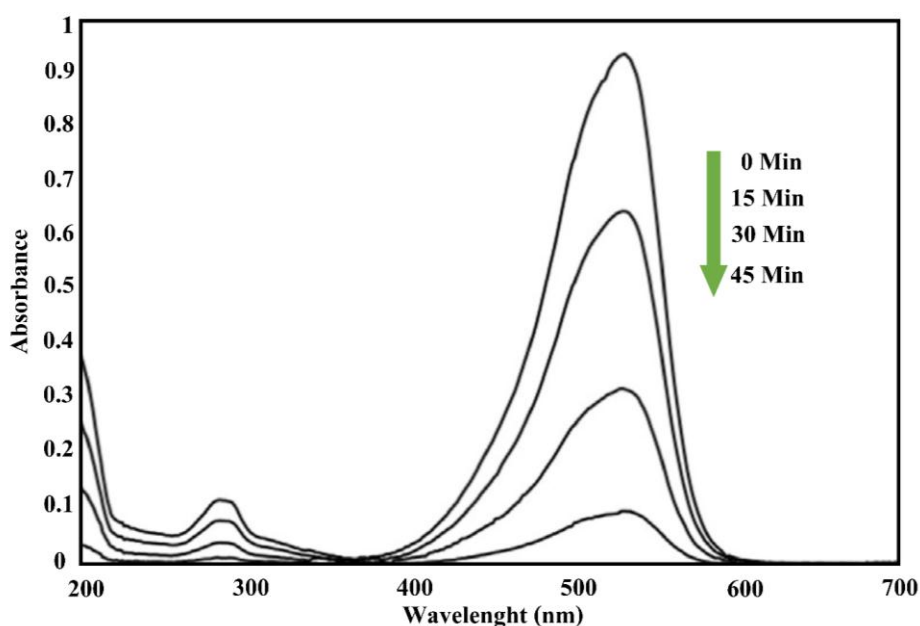


Fig. 9. UV-vis spectral changes of AO7 during photocatalytic degradation in the presence of Zn-TiO₂ nanoparticles

Absorption spectra of AO7 solution declined during photocatalytic degradation. The decrease in the absorption peak of AO7 at $\lambda = 530$ nm indicates a rapid degradation of dye. The decrease is also meaningful with respect to the nitrogen-to-nitrogen double bond ($-\text{N} = \text{N}-$) of azo dye, as the most active site for oxidative attack. The absorbance of AO7 at $\lambda = 254$ nm is responsible for aromatic ring content attached to the $-\text{N} = \text{N}-$ group in the AO7 molecular structure. The disappearance of AO7 aromatic ring content in the aqueous solution was measured, using the band intensity at 254 nm after 30 min irradiation time and results showed 78.82% reduction at 254 nm absorbance intensity, indicative of degradation and mineralization of AO7 aromatic ring.

CONCLUSION

Zn-TiO₂ compounds were prepared in the presence of Green Tea as a green reducing agent. The byproducts were characterized, using XRD, FESEM, EDS, and DRS. Zn-TiO₂ compound with 25wt% Zn showed higher photocatalytic performance in photodegradation of AO7 than bare TiO₂. In order to investigate the presence of Zn, different weight ratios of Zn to TiO₂ (5wt%, 10wt%, 15wt%, 20wt%, 25wt%, 30wt%, 35wt%, 40wt%, 45wt%, and 50wt%) were synthesized and their performance in AO7 photodegradation was compared with pure TiO₂. According to the results, 25wt% Zn-loaded TiO₂ nanoparticle exhibited high photocatalytic activity for the degradation of AO7 dye. Results showed that the significant enhancement in photodegradation efficiency of AO7 degradation was due to the presence of Zn metal, which possessed effective charge carrier separation properties. Finally, results clearly emphasized that AO7 degradation mainly depended on photogenerated holes only.

ACKNOWLEDGEMENT

Authors are grateful to Council of the University of Tehran for providing financial support to undertake this work.

REFERENCES

- Ayni, S., Sabet, M. and Salavati-Niasari, M. (2016) Synthesis and Characterization of Lead Molybdate Nanostructures with High Photocatalytic Activity Via Simple Co-precipitation Method. *Journal of Cluster Science.*, 27(1); 315-326.
- Eskandarloo, H., Badiei, A. and Haug, C. (2014). Enhanced photocatalytic degradation of an azo textile dye by using TiO₂/NiO coupled nanoparticles: Optimization of synthesis and operational key factors. *Mater. Sci. Semicond. Process.*, 27(1); 240-253.
- Eskandarloo, H., Badiei, A., Behnajadi, M. A. and Mohammadi Ziarani, G. (2016a). Ultrasonic-assisted degradation of phenazopyridine with a combination of Sm-doped ZnO nanoparticles and inorganic oxidants. *Ultrason Sonochem.*, 28(1); 169-177.
- Eskandarloo, H., Badiei, A., Behnajadi, M. A., Tavakoli, A. and Mohammadi Ziarani, G. (2016b). Ultrasonic-assisted synthesis of Ce doped cubic-hexagonal ZnTiO₃ with highly efficient sonocatalytic activity. *Ultrason Sonochem.*, 29(1); 258-269.
- Fujishima, A., Zhang, X. and Tryk, D. A. (2008). TiO₂ photocatalysis and related surface phenomena. *Surf Sci.*, 63(12); 515-582.
- Hashimoto, K., Irie, H. and Fujishima, A. (2005). TiO₂ Photocatalysis: A Historical Overview and Future Prospects. *Jpn J Appl Phys.*, 44(12); 8269-8285.
- Huang, Q., Tian, S., Zeng, D., Wang, X., Song, W., Li, Y., Xiao, W. and Xie, C. (2013). Enhanced Photocatalytic Activity of Chemically Bonded TiO₂/Graphene Composites Based on the Effective Interfacial Charge Transfer through the C-Ti Bond. *ACS Catal.*, 3(7); 1477-1485.
- Lin, J. and Zhu, Y. F. (2007). Controlled Synthesis of the ZnWO₄ Nanostructure and Effects on the Photocatalytic Performance. *Inorg. Chem.*, 46(20); 8372-8378.
- Malato, S., Fernández-Ibáñez, P., Maldonado, M. I., Blanco, J. and Gernjak, W. (2009). Decontamination and disinfection of water by solar photocatalysis: Recent overview and trends. *Catal Today.*, 147(1); 1-59.

- Masoumi, S., Nabiyouni, G. and Ghanbari, D. (2016). Photo-degradation of Congo red, acid brown and acid violet: photo catalyst and magnetic investigation of $\text{CuFe}_2\text{O}_4\text{-TiO}_2\text{-Ag}$ nanocomposites. *J. Mater. Sci. - Mater. Electron.*, 27(10); 11017-11033.
- Nayak, J., Lohani, H., Bera, T.K. (2011). Observation of catalytic properties of CdS–ZnO composite nanorods synthesized by aqueous chemical growth technique. *Curr. Appl. Phys.*, 11(1); 93-97.
- Neelakandeswari, N., Sangami, G., Dharmaraj, N., Taek, N. K. and Kim, H. Y. (2011). Spectroscopic investigations on the photodegradation of toluidine blue dye using cadmium sulphide nanoparticles prepared by a novel method. *Spectrochim. Acta, Part A.*, 78(5); 1592-1598.
- Roig, B., Gonzalez, C. and Thomas, O. (2003). Monitoring of phenol photodegradation by ultraviolet spectroscopy. *Spectrochim. Acta, Part A.*, 59(2); 303-307.
- Sabet, M. and Salavati-Niasari, M. (2015). Deposition of Lead Sulfide Nanostructure Films on TiO_2 Surface via Different Chemical Methods due to Improving Dye-Sensitized Solar Cells Efficiency. *Electrochimica Acta.*, 169(1); 168-179.
- Sabet, M., Jahangiri, H. and Ghashghaei, E. (2017). Improving microwave absorption of the polyaniline by carbon nanotube and needle-like magnetic nanostructures. *Synthetic Metals.*, 224(1); 18-26.
- Sabet, M., Salavati-Niasari, M., Ashjari, M., Ghanbari, D. and Dadkhah, M. (2012). $\text{CuInS}_2/\text{CuS}$ Nanocomposite: Synthesis via Simple Microwave Approach and Investigation Its Behavior in Solar Cell. *Journal of Inorganic and Organometallic Polymers and Materials.*, 22(5); 1139-1145.
- Sabet, M., Salavati-Niasari, M., Ghanbari, D., Amiri, O., Mir, N. and Dadkhah, M. (2014). Synthesis and characterization of CuInSe_2 nanocrystals via facile microwave approach and study of their behavior in solar cell. *Materials Science in Semiconductor Processing.*, 25(1); 98-105.
- Sangsefidi, F. S., Sabet, and Salavati-Niasari, M. (2016) Synthesis and characterization of ceria nanostructures with different morphologies via a simple thermal decompose method with different cerium complexes and investigation the photocatalytic activity. *Journal of Materials Science: Materials in Electronics.*, 27(8); 8793-8801.
- Shen, J., Hu, Y., Shi, M., Li, N., Ma, H. and Ye, M. (2010). One Step Synthesis of Graphene Oxide–Magnetic Nanoparticle Composite. *J. Phys. Chem. C.*, 114(3); 1498-1503.
- Shiravand, G., Badiei, A., Mohammadi Ziarani, G., Jafarabadi, M. and Hamzehloo, M. (2012). Photocatalytic Synthesis of Phenol by Direct Hydroxylation of Benzene by a Modified Nanoporous Silica (LUS-1) under Sunlight. *Chin. J. Catal.*, 33(7-8); 1347-1353.
- Tavakoli, F., Salavati Niasari, M. and Mohandes, F. (2013). Green synthesis of flower-like CuI microstructures composed of trigonal nanostructures using pomegranate juice. *Mater. Lett.*, 100(1); 133-136.
- Tavakoli, F., Salavati Niasari, M., Badiei, A. and Mohandes, F. (2015). Green synthesis and characterization of graphene nanosheets. *Mater. Res. Bull.*, 63(1); 51-57.
- Wang, X., Hu, P., Li, Y.F. and Yu, L. (2007). Preparation and Characterization of ZnO Hollow Spheres and ZnO –Carbon Composite Materials Using Colloidal Carbon Spheres as Templates. *J. Phys. Chem. C.*, 111(18); 6706-6712.
- Xie, W., Li, Y., Sun, W., Huang, J., Xie, H. and Zhao, X. (2010). Surface modification of ZnO with Ag improves its photocatalytic efficiency and photostability. *J. Photochem. Photobiol., A. Chem.*, 216(2-3); 149-155.
- Xu, T., Zhang, L., Cheng, H. and Zhu, Y. (2011). Significantly enhanced photocatalytic performance of ZnO via graphene hybridization and the mechanism study. *Appl. Catalysis B: Environ.*, 101(3-4); 382-387.

